Carbaborane Derivatives of the Late- and Post-transition Elements. Part 2.† Dicarbaundecaboranyl Compounds of Copper(I), Gold(I), and Mercury(II); the Crystal and Molecular Structure of 3-Triphenylphosphine-3-mercura-1,2-dicarbadodecaborane(II), a Pseudo-σ-bonded Metallacarbaborane

By **Howard M. Colquhoun, Trevor J. Greenhough,** and **Malcolm G. H. Wallbridge,*** Department of Chemistry and Molecular Sciences, University of Warwick, Coventry CV4 7AL

The novel d^{10} metallacarbaboranes $B_9C_2^{1,2}[Hg(PPh_3)]^3H_{11}$ (1), $[AsPh_4][B_9C_2^{1,2}(HgMe)^3H_{11}]$, $B_9C_2^{1,2}[Au(PPh_3)]^3(NC_5H_5)^4H_{10}$, $B_9C_2^{1,2}[Cu(PPh_3)]^3(NC_5H_5)^4H_{10}$, and $[3,3'\text{-}\{Hg[B_9C_2^{1,2}(NC_5H_5)^4H_{10}\}_2]$ have been prepared by reactions of $[\{HgCl_2(PPh_3)\}_2]$ with $Tl[B_9C_2^{1,2}Tl^3H_{11}]$, $[HgMe(O_2CMe)]$ with aqueous $K[B_9C_2H_{12}]$–K[OH], and $Na[B_9C_2^{7,8}(NC_5H_5)^9H_{10}]$ with $[AuCl(PPh_3)]$, $[\{CuCl(PPh_3)\}_4]$, and $HgCl_2$ respectively. The molecular structure of compound (1), as the 0.5-dioxan solvate, has been determined at −60 °C, and shows the mercury atom to be co-ordinated almost linearly by PPh_3 and the unique boron atom of the C_2B_3 face, implying a direct mercury–boron σ bond (Hg–B 2.20, Hg–P 2.39 Å, P–Hg–B 172°). The crystals are triclinic, space group $P\bar{1}$ with cell dimensions a = 10.913 5(17), b = 11.188 3(19), c = 12.007 1(18) Å, α = 83.50(1), β = 86.98(1), γ = 61.55(1)°, and Z = 2, and the structure has been refined to R = 0.037 for 2 447 independent observed reflections.

THE incorporation of 'electron-rich' (d^8—$d^{10}s^2$) metal ions, such as those of the Ni–Pd–Pt, Cu–Ag–Au, Zn–Cd–Hg, and Ga–In–Tl triads, into the open C_2B_3 face of the $[B_9C_2H_{11}]^{2-}$ ion to yield metallacarbaboranes has already been reported for several d^8 (Ni^{II}, Pd^{II}, Pt^{II}, Cu^{III}, and Au^{III}),[1-5] d^9 (Cu^{II} and Au^{II}),[1,4] and $d^{10}s^2$ (Tl^I)[6] ions. Compounds containing the d^8 and d^9 ions have been described as adopting the 'slipped' configuration where the metal apparently slips across a planar C_2B_3 face of the $[B_9C_2H_{11}]^{2-}$ ligand, although recent structural results for the d^8 species $B_9C_2^{1,2}[Au(S_2CNEt_2)]H_{11}$,[5] $[Au(S_2CNEt_2)_2][Au(B_9C_2^{1,2}H_{11})_2]$,[7] and $B_9C_2^{1,2}[Pt(PEt_3)_2]H_{11}$[3] have shown that the molecular distortions are associated particularly with a bending of the open C_2B_3 face, by up to 17°, and the lengthening of the B–C (facial) bonds. As part of an investigation into the co-ordination behaviour of carbaborane anions with electron-rich metal ions, we have studied the reactions between *nido*-dicarbaundecaborate ions $\{[B_9C_2^{7,8}H_{11}]^{2-}$ and $[B_9C_2^{7,8}(NC_5H_5)^9H_{10}]^-\}$ and a series of compounds of Hg^{II}, Au^I, and Cu^I, and now report the characterisation of the resulting d^{10} metallacarbaboranes. The only reported d^{10} compound in this series to date is $[B_9C_2(HgPh)H_{11}]^-$,[8] formed by the action of $Na_2[B_9C_2^{7,8}H_{11}]$ on [HgPhCl], in which the presence of a mercury–cage-carbon σ bond was proposed. Preliminary *X*-ray structural details for one of the compounds reported here, $B_9C_2^{1,2}[Hg(PPh_3)]^3H_{11}$,[9] have been given previously.

† Part 1 is ref. 25.

RESULTS AND DISCUSSION

The reaction between $[\{HgCl_2(PPh_3)\}_2]$ and $Tl[B_9C_2^{1,2}Tl^3H_{11}]$[6] in tetrahydrofuran (thf) or dichloromethane at room temperature yields a colourless, moderately air-stable, crystalline compound, $B_9C_2^{1,2}[Hg(PPh_3)]^3H_{11}$ (1) which crystallises from 1,4-dioxan–acetone–diethyl ether as the 0.5-dioxan solvate (1a). An analogous methylmercury derivative is obtained by reaction of aqueous $K[B_9C_2^{7,8}H_{12}]$ with $[HgMe(O_2CMe)]$ in the presence of strong base (K[OH]), and may be precipitated as the tetraphenylarsonium salt $[AsPh_4][B_9C_2(HgMe)H_{11}]$ (2). The known phenylmercury compound $[NMe_4][B_9C_2^{1,2}(HgPh)^3H_{11}]$ (2a) was prepared by the interaction of $[HgPh(NO_3)]$ and $Tl[B_9C_2^{1,2}Tl^3H_{11}]$ followed by precipitation of the anion from aqueous solution using $[NMe_4]Br$.

TABLE 1

Hydrogen-1 and ^{11}B n.m.r. data *

	Compound	^1H [δ(SiMe$_4$) = 0]	^{11}B (all doublets unless otherwise stated) [δ(OEt$_2$·BF$_3$) = 0]
(1)	$B_9C_2[Hg(PPh_3)]H_{11}$	7.74 (m, 15 H), 1.89 (s, br, 2 H) (in CD_2Cl_2)	−13.36 (2 B), −16.2 (4 B), −19.96 (1 B), −24.02 (1 B), −32.30 (1 B) (in Me_2CO)
(2)	$[AsPh_4][B_9C_2(HgMe)H_{11}]$	7.72 (m, 20 H), 1.52 (s, br, 2 H), 0.62 [s, 3 H, J (^{199}Hg–CH_3) 145 Hz] (in CD_3CN)	−15.14 (5 B), −21.99 (3 B), −35.09 (1 B) (in Me_2CO)
(2a)	$[NMe_4][B_9C_2(HgPh)H_{11}]$		−16.07 (5 B), −21.65 (2 B), −24.44 (1 B), −34.84 (1 B) (in Me_2CO)
(3)	$B_9C_2[Au(PPh_3)](NC_5H_5)H_{10}$		−1.86 (s, 1 B), −12.18 (1 B), −18.10 (4 B), −23.17 (2 B), −35.94 (1 B) (in Me_2CO)
(4)	$B_9C_2[Cu(PPh_3)](NC_5H_5)H_{10}$	8.74 (m, 2 H), 8.15 (m, 1 H), 7.52 (m, 16 H), 3.05 (s, br, 1 H), 1.90 (s, br, 1 H)	−5.24 (s, 1 B s), −15.48 (2 B), −21. 23 (4 B), −25.88 (1 B), −34.08 (1 B) (in Me_2CO)
(5)	$[Hg\{B_9C_2(NC_5H_5)H_{10}\}_2]$	9.04 (m, 2 H), 8.50 (m, 1 H), 8.00 (m, 2 H), 2.85 (s, br, 1 H), 1.65 (s, br, 1 H) [in $(CD_3)_2SO$]	0.34 (s, 1 B), −8.96 (1 B), −19.20 (6 B), −35.80 (1 B) (in Me_2CO–Me_2SO)

* Recorded at 90 (^1H) and 28.9 MHz (^{11}B) using a Bruker WH90 spectrometer. Downfield ^1H and ^{11}B shifts are given as positive.

Similar compounds of Group 1B metals with the monoanion $[B_9C_2^{7,8}(NC_5H_5)^9H_{10}]^-$ (ref. 10) resulted from reactions in thf solution between $Na[B_9C_2^{7,8}(NC_5H_5)^9H_{10}]$ and $[AuCl(PPh_3)]$ and $[\{CuCl(PPh_3)\}_4]$, which gave $B_9C_2^{1,2}[Au(PPh_3)]^3(NC_5H_5)^4H_{10}$ (3), and $B_9C_2^{1,2}[Cu(PPh_3)]^3(NC_5H_5)^4H_{10}$ (4), respectively, as bright yellow air-stable crystalline solids. The corresponding mercury(II) derivative, $[3,3'\text{-}Hg\{B_9C_2^{1,2}(NC_5H_5)^4H_{10}\}_2]$ (5), was also obtained as a pale yellow microcrystalline powder by treating $HgCl_2$ with the sodium carbaborane salt, $Na[B_9C_2(NC_5H_5)H_{10}]$.

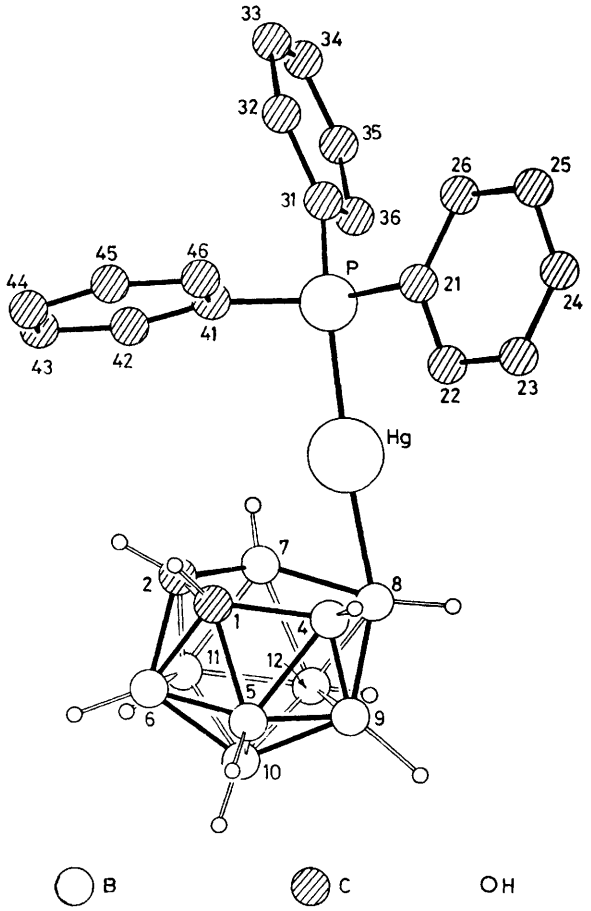

FIGURE 1 Molecular structure of $B_9C_2^{1,2}[Hg(PPh_3)]^3H_{11}$. Phenyl hydrogen atoms are omitted

The various compounds may be partially characterised from their spectroscopic properties. Thus, in the ^1H n.m.r. spectra of the $[B_9C_2H_{11}]^{2-}$ derivatives (1) and (2) the CH carbaborane protons are equivalent and appear as singlets near 1.5—2 p.p.m. (Table 1), while in the $B_9C_2(NC_5H_5)H_{10}$ compounds (3)—(5) the lack of any plane of symmetry due to the presence of the pyridine molecule causes the singlet to be split into two signals at 1.5—3 p.p.m. The signals from the various aromatic protons occur near 8 p.p.m., and as expected the remaining BH protons cannot be clearly identified due to coupling with the ^{11}B nucleus ($I = \frac{3}{2}$) and extensive quadrupole broadening. The ^{11}B n.m.r.

TABLE 2

Final atomic co-ordinates ($\times 10^4$, Hg $\times 10^5$) for the non-hydrogen atoms with standard deviations in parentheses

Atom	*x*	*y*	*z*
Hg	36 202(4)	40 347(4)	06 954(3)
P	3 419(2)	3 747(2)	2 691(2)
C(1)	3 543(12)	1 956(10)	−0 485(8)
C(2)	2 130(11)	3 232(11)	−0 740(9)
B(4)	4 852(13)	2 245(14)	−0 620(10)
B(5)	4 523(15)	1 423(14)	−1 659(10)
B(6)	2 720(15)	2 039(13)	−1 704(11)
B(7)	2 194(15)	4 625(14)	−1 061(11)
B(8)	4 105(15)	4 086(14)	−1 109(9)
B(9)	4 838(18)	2 802(21)	−2 041(12)
B(10)	3 518(15)	2 725(14)	−2 712(10)
B(11)	1 909(15)	3 767(14)	−2 114(10)
B(12)	3 167(18)	4 329(14)	−2 333(11)
C(21)	5 103(9)	3 065(9)	3 330(7)
C(22)	6 249(11)	2 118(11)	2 770(8)
C(23)	7 566(11)	1 564(11)	3 209(9)
C(24)	7 751(10)	1 911(10)	4 207(9)
C(25)	6 640(11)	2 838(10)	4 780(8)
C(26)	5 325(10)	3 398(9)	4 344(8)
C(31)	2 151(9)	5 271(8)	3 300(7)
C(32)	1 608(10)	5 186(10)	4 347(8)
C(33)	0 551(11)	6 341(12)	4 740(9)
C(34)	0 045(11)	7 564(10)	4 089(10)
C(35)	0 585(12)	7 660(10)	3 049(9)
C(36)	1 638(10)	6 524(9)	2 656(8)
C(41)	2 815(10)	2 490(9)	2 996(7)
C(42)	1 639(10)	2 691(10)	2 468(8)
C(43)	1 157(13)	1 757(14)	2 655(10)
C(44)	1 857(13)	0 611(12)	2 395(10)
C(45)	3 047(12)	0 372(11)	3 928(10)
C(46)	3 497(11)	1 347(10)	3 741(8)
O	−0 135(8)	0 413(9)	1 084(6)
C(51)	1 204(12)	−0 319(14)	0 584(10)
C(52)	−1 132(12)	1 176(13)	0 235(10)

TABLE 3

Final positional parameters (fractional co-ordinates $\times 10^3$) for the hydrogen atoms with estimated standard deviations in parentheses

Atom	*x*	*y*	*z*
H(1)	343(10)	121(10)	004(8)
H(2)	124(12)	322(10)	−061(8)
H(4)	591(11)	160(11)	−012(9)
H(5)	517(12)	016(11)	−174(9)
H(6)	223(11)	142(11)	−188(9)
H(7)	117(11)	593(10)	−094(8)
H(8)	483(10)	462(10)	−125(8)
H(9)	576(13)	283(12)	−263(10)
H(10)	340(11)	262(10)	−356(8)
H(11)	115(12)	408(11)	−257(9)
H(12)	302(12)	532(11)	−278(9)
H(22)	593(11)	208(10)	209(8)
H(23)	827(10)	097(10)	287(8)
H(24)	866(10)	151(10)	457(8)
H(25)	687(10)	297(10)	552(8)
H(26)	447(10)	404(9)	482(8)
H(32)	196(10)	424(9)	480(7)
H(33)	011(11)	637(10)	539(8)
H(34)	−051(11)	823(10)	427(8)
H(35)	042(11)	835(10)	256(8)
H(36)	196(10)	661(9)	199(8)
H(42)	136(10)	332(10)	205(8)
H(43)	015(11)	181(11)	218(9)
H(44)	166(12)	−004(11)	346(9)
H(45)	383(11)	−072(11)	453(9)
H(46)	430(10)	122(10)	400(8)
H(511)	109(12)	065(11)	011(9)
H(512)	203(12)	−097(11)	124(9)
H(521)	−208(13)	177(12)	053(10)
H(522)	−095(12)	181(12)	−017(10)

spectra (Table 1) show a series of doublet signals but, apart from being consistent with the presence of nine boron atoms, the difficulty of making assignments of individual boron atoms is increased by extensive overlap, and even in (3)—(5), where some separation of signals might be expected, line-narrowed ^{1}H-decoupled spectra failed to resolve all the individual signals. The ^{11}B spectra of (1), (2), and (2a) are different in form from those of (3)—(5), the latter all showing a singlet resonance due to the pyridine-substituted B atom at low field, but it is noteworthy that none of the spectra shows the one-boron doublet at lower field which is frequently associated with ' slipped ' structures.[4]

In order to determine the precise nature of the metal–cage interaction, a single-crystal *X*-ray study of the dioxan solvate (1a) was undertaken; the structure of the $B_9C_2^{1,2}[Hg(PPh_3)]^3H_{11}$ molecule, determined at −60 °C,

TABLE 4

Bond lengths (Å) with estimated standard deviations in parentheses

Hg–B(4)	2.50(1)	C(1)–C(2)	1.54(1)
Hg–B(7)	2.52(1)	C(1)–B(4)	1.61(2)
Hg–B(8)	2.20(1)	C(2)–B(7)	1.60(2)
Hg–C(1)	2.89(1)	B(7)–B(8)	1.87(2)
Hg–C(2)	2.91(1)	B(4)–B(8)	1.85(2)
C(1)–B(6)	1.73(2)	B(9)–B(12)	1.83(2)
C(1)–B(5)	1.71(2)	B(12)–B(11)	1.76(3)
C(2)–B(6)	1.73(2)	B(11)–B(6)	1.72(2)
C(2)–B(11)	1.68(2)	B(6)–B(5)	1.75(2)
B(7)–B(11)	1.79(2)	B(5)–B(9)	1.74(3)
B(7)–B(12)	1.78(2)	B(10)–B(12)	1.76(2)
B(4)–B(9)	1.75(2)	B(10)–B(11)	1.75(2)
B(4)–B(5)	1.78(2)	B(10)–B(6)	1.77(2)
B(8)–B(12)	1.76(2)	B(10)–B(5)	1.77(2)
B(8)–B(9)	1.77(2)	B(10)–B(9)	1.73(3)
Hg–P	2.393(2)	C(31)–C(32)	1.37(1)
P–C(21)	1.797(10)	C(32)–C(33)	1.37(1)
P–C(31)	1.813(8)	C(33)–C(34)	1.37(2)
P–C(41)	1.813(12)	C(34)–C(35)	1.37(2)
		C(35)–C(36)	1.36(1)
C(21)–C(22)	1.40(1)	C(36)–C(31)	1.39(1)
C(22)–C(23)	1.37(2)		
C(23)–C(24)	1.36(2)	C(41)–C(42)	1.37(2)
C(24)–C(25)	1.38(1)	C(42)–C(43)	1.37(2)
C(25)–C(26)	1.37(1)	C(34)–C(44)	1.38(2)
C(26)–C(21)	1.38(1)	C(44)–C(45)	1.37(2)
		C(45)–C(46)	1.39(2)
O–C(51)	1.43(1)	C(46)–C(41)	1.38(1)
O–C(52)	1.41(1)		
C(51)–C(52)	1.48(2)	C(22)–H(22)	0.9(1)
		C(23)–H(23)	0.8(1)
C(1)–H(1)	1.0(1)	C(24)–H(24)	1.0(1)
C(2)–H(2)	1.0(1)	C(25)–H(25)	1.0(1)
B(4)–H(4)	1.2(1)	C(26)–H(26)	1.1(1)
B(5)–H(5)	1.3(1)		
B(6)–H(6)	1.1(1)	C(32)–H(32)	1.0(1)
B(7)–H(7)	1.4(1)	C(33)–H(33)	0.9(1)
B(8)–H(8)	1.2(1)	C(34)–H(34)	0.8(1)
B(9)–H(9)	1.2(1)	C(35)–H(35)	0.9(1)
B(10)–H(10)	1.1(1)	C(36)–H(36)	0.9(1)
B(11)–H(11)	0.9(1)		
B(12)–H(12)	1.1(1)	C(42)–H(42)	0.8(1)
		C(43)–H(43)	1.2(1)
C(51)–H(511)	1.1(1)	C(44)–H(44)	0.8(1)
C(51)–H(512)	1.1(1)	C(45)–H(45)	1.3(1)
C(52)–H(521)	1.0(1)	C(46)–H(46)	0.9(1)
C(52)–H(522)	0.9(1)		

is shown in Figure 1, the one molecule of dioxan per unit cell being present as non-co-ordinated lattice solvent.

Description of the Structure.—Final atomic positional parameters for the non-hydrogen atoms are given in

TABLE 5

Interbond angles (°) with estimated standard deviations in parentheses

(*a*) Within the polyhedron

C(2)–Hg–C(1)	30.7(3)	C(1)–B(5)–B(4)	54.8(8)
C(2)–Hg–B(7)	33.2(5)	B(4)–B(5)–B(9)	59.5(9)
C(1)–Hg–B(4)	33.6(5)	B(9)–B(5)–B(10)	59.0(9)
B(4)–Hg–B(8)	45.9(5)	B(10)–B(5)–B(6)	60.3(8)
B(7)–Hg–B(8)	46.1(5)	B(6)–B(5)–C(1)	60.0(8)
Hg–C(1)–B(4)	59.6(6)	C(2)–B(6)–C(1)	52.8(6)
Hg–C(2)–B(7)	59.9(7)	C(1)–B(6)–B(5)	58.8(8)
Hg–C(1)–C(2)	75.2(7)	B(5)–B(6)–B(10)	60.4(8)
Hg–C(2)–C(1)	74.1(7)	B(10)–B(6)–B(11)	60.2(8)
Hg–B(4)–C(1)	86.8(6)	B(11)–B(6)–C(2)	58.2(7)
Hg–B(7)–C(2)	86.9(6)		
Hg–B(7)–B(8)	58.0(5)	B(8)–B(9)–B(4)	63.5(8)
Hg–B(7)–B(8)	58.0(5)	B(4)–B(9)–B(5)	61.2(10)
Hg–B(4)–B(8)	58.7(5)	B(5)–B(9)–B(10)	61.3(11)
Hg–B(8)–B(4)	75.5(6)	B(10)–B(9)–B(12)	59.2(9)
Hg–B(8)–B(7)	75.9(10)	B(12)–B(9)–B(8)	58.5(8)
C(1)–C(2)–B(6)	63.6(7)	B(6)–B(10)–B(11)	58.6(8)
B(6)–C(1)–C(2)	63.6(7)	B(11)–B(10)–B(12)	60.2(10)
B(4)–C(1)–B(5)	64.8(9)	B(12)–B(10)–B(9)	63.1(10)
B(7)–C(2)–B(11)	66.4(9)	B(9)–B(10)–B(5)	59.7(10)
B(5)–C(1)–B(6)	61.2(8)	B(5)–B(10)–B(6)	59.3(8)
B(11)–C(2)–B(6)	60.7(7)		
B(5)–B(4)–C(1)	60.4(9)	C(2)–B(11)–B(7)	54.6(8)
B(11)–B(7)–C(2)	59.1(9)	B(7)–B(11)–B(12)	60.2(9)
B(9)–B(4)–B(5)	59.3(11)	B(12)–B(11)–B(10)	60.1(9)
B(12)–B(7)–B(11)	58.9(9)	B(10)–B(11)–B(6)	61.2(8)
B(8)–B(4)–B(9)	58.8(9)	B(6)–B(11)–C(2)	61.1(7)
B(8)–B(7)–B(12)	57.3(8)		
B(7)–B(8)–B(12)	58.7(8)	B(7)–B(12)–B(8)	63.9(8)
B(4)–B(8)–B(9)	57.6(8)	B(8)–B(12)–B(9)	59.2(8)
B(12)–B(8)–B(9)	62.3(8)	B(9)–B(12)–B(10)	57.7(10)
		B(10)–B(12)–B(11)	59.7(9)
C(2)–C(1)–B(4)	114(1)	B(11)–B(12)–B(7)	60.8(10)
C(1)–C(2)–B(7)	115(1)		
C(2)–B(7)–B(8)	104(1)	B(12)–B(9)–B(5)	108(1)
C(1)–B(4)–B(8)	105(1)	B(9)–B(12)–B(11)	105(1)
B(4)–B(8)–B(7)	101(1)	B(12)–B(11)–B(6)	110(1)
		B(9)–B(5)–B(6)	108(1)
		B(5)–B(6)–B(11)	109(1)

(*b*) Exo-polyhedral bond angles

C(21)–C(22)–C(23)	120.9(10)	C(41)–C(42)–C(43)	120.9(9)
C(22)–C(23)–C(24)	119.2(9)	C(42)–C(43)–C(44)	119.3(13)
C(23)–C(24)–C(25)	121.1(10)	C(43)–C(44)–C(45)	121.2(15)
C(24)–C(25)–C(26)	119.5(10)	C(44)–C(45)–C(46)	118.2(10)
C(25)–C(26)–C(21)	120.9(8)	C(45)–C(46)–C(41)	121.1(11)
C(26)–C(21)–C(22)	118.3(9)	C(46)–C(41)–C(42)	119.2(11)
C(31)–C(32)–C(33)	119.5(9)	P–C(21)–C(22)	117.6(8)
C(32)–C(33)–C(34)	119.9(10)	P–C(21)–C(26)	124.1(6)
C(33)–C(34)–C(35)	121.0(9)	P–C(31)–C(32)	120.9(7)
C(34)–C(35)–C(36)	119.5(9)	P–C(31)–C(36)	119.0(7)
C(35)–C(36)–C(31)	120.2(9)	P–C(41)–C(42)	118.7(7)
C(36)–C(31)–C(32)	119.8(7)	P–C(41)–C(46)	122.1(9)
C(21)–P–Hg	109.9(3)	C(21)–P–C(31)	111.3(5)
C(31)–P–Hg	114.4(3)	C(31)–P–C(41)	106.3(4)
C(41)–P–Hg	106.7(3)	C(41)–P–C(21)	107.8(4)
P–Hg–B(8)	172.2(3)	C(51)–O–C(52)	109.3(8)
		O–C(51)–C(52)	109.5(12)
		O–C(52)–C(51)	112.9(10)

Table 2 with least-squares estimated standard deviations, the hydrogen-atom positional parameters are in Table 3. Bond distances and angles are given in Tables 4 and 5, the atomic numbering scheme in Figure 1, and equations

of some best least-squares planes in Table 6. Hydrogen atoms are numbered according to the number of the carbon or boron to which they are bonded except for those in the dioxan of solvation where H(511) and H(512) are bonded to C(51), and H(521) and H(522) to C(52).

TABLE 6

Some best least-squares planes expressed in the form $PI + QJ + RK = S$ (orthogonal Å space)

	Plane (1)	Plane (2)	Plane (3)	Plane (4)	Plane (5)	Plane (6)	Plane (7)
P	0.046 6	0.121 5	0.670 6	−0.575 1	0.524 6	0.886 6	−0.335 2
Q	0.161 3	0.208 9	0.181 0	−0.810 0	0.747 0	0.184 8	0.4884
R	0.985 8	0.970 4	0.981 2	0.114 4	−0.408 4	0 424 1	0.805 7
S	0.145 5	0.737 3	−1 182 6	0.443 3	4.369 3	7.614 4	2.751 8
Atoms defining the plane (unit weight) and distances (Å) from the plane	C(1) 0.008 C(2) −0.008 B(4) −0.004 B(7) 0.005	B(4) 0 B(7) 0 B(8) 0	B(5) −0.001 B(9) −0.001 B(11) −0.005 B(13) 0.004 B(6) 0.004	B(8) 0 B(6) 0 B(10) 0	C(21) 0.006 C(22) −0.001 C(23) −0.003 C(24) 0.002 C(25) 0.003 C(26) −0.007	C(31) −0.005 C(32) 0.001 C(33) 0.003 C(34) −0.003 C(35) −0.001 C(36) 0.005	C(41) −0.007 C(42) 0.001 C(43) −0.001 C(44) 0.008 C(45) −0.014 C(46) 0.014
σ	0.008	0	0.004	0	0.005	0.004	0.010
Other atoms and distances (Å) from the plane	Hg 1.993 B(8) −0.107 H(1) 0.415 H(2) 0.099 H(4) 0.466 H(7) 0.465	Hg 2.030 H(4) 0.495 H(7) 0.485 H(8) 1.125	Hg 3.522 H(5) −0.427 H(9) −0.504 H(11) −0.233 H(12) −0.618 H(6) −0.435	Hg 0.033 P 0.390 B(4) 1.428 B(7) −1.447 C(1) 0.768 C(2) −0.770 B(5) 1.432 B(11) −1.401 B(9) 0.908 B(12) −0.917	H(22) 0.091 H(23) −0.005 H(24) −0.028 H(25) −0.072 H(26) −0.093 P −0.005	H(32) −0.055 H(33) −0.032 H(34) 0.021 H(35) 0.053 H(36) 0.008 P −0.182	H(42) −0.057 H(43) −0.061 H(44) −0.106 H(45) −0.148 H(46) −0.083 P −0.041
Acute angles (°) between the planes	(1)–(2) 5.2 (1)–(3) 1.7 (1)–(4) 89.5	(2)–(3) 3.5 (2)–(4) 89.3 (3)–(4) 89.7					

The accuracy of the structure determination has undoubtedly suffered from the incompleteness of the data set, the reflection-to-variable ratio being only 6.1 : 1. Furthermore, marked trends in the agreement between $|F_o|$ and $|F_c|$ suggest that absorption varies significantly with crystal orientation; trends in $w\Delta F$, however, are less marked suggesting that absorption has in part been accounted for by the weightings employed. In spite of these shortcomings in the data, all the hydrogen atoms have been located and positionally refined, generally adopting acceptable positions, and the refinement has been brought to a satisfactory conclusion.

The C_2B_9 *framework.* The carbaborane cage exhibits mirror symmetry to within experimental error; apart from the bond distances of the open C_2B_3 face, there are no significant (3σ) differences between the interatomic separations in the $B_9C_2^{1,2}$ cage here and in other structural determinations of the $B_9C_2^{1,2}M^3H_{11}$ fragment.

The C–C distance lies midway between the two known extremes of 1.46(2) Å in $B_9C_2^{1,2}[Au(S_2CNEt_2)]^3H_{11}$ (ref. 5) and 1.61(2) Å in the symmetrically bonded $[B_9C_2^{1,2}\{Re(CO)_3\}^3H_{11}]^-$ (refs. 11 and 12) and differs significantly from both. The facial B–B separations differ significantly from those in the symmetrically bonded nickel(III) analogue $[NMe_4][3,3'\text{-}Ni^{III}(B_9C_2H_{11})_2]$ [1.769(8), 1.769(8) Å],[13] the asymmetry of these distances in $[B_9C_2^{1,2}\{Re(CO)_3\}^3H_{11}]^-$ [1.76(2), 1.81(2) Å] not allowing a useful comparison. The facial B–C bond distances are the shortest known examples of such bonds in $B_9C_2^{1,2}M^3$ fragments. Other than those found here, the known range is from 1.67(1), 1.71(1) Å in the copper(II) (d^9) anion $[3,3'\text{-}Cu(B_9C_2^{1,2}H_{11})_2]^{2-}$,[14] to 1.81(2), 1.82(2) Å in the highly distorted gold(III) (d^8) compound $B_9C_2^{1,2}[Au(S_2CNEt_2)]^3H_{11}$.[5]

Unlike the structurally characterised d^8 and d^9 $B_9C_2^{1,2}M^3$ metallacarbaboranes, which show distinct non-planarity of both the C_2B_3 face and the lower B_5 pentagonal girdle, this d^{10} compound is similar to the symmetrically bonded d^6, d^7 derivatives in that only small deviations from planarity, not significant here in the case of the lower B_5 plane, are present.

The average B–H bond distance is 1.17 Å and there are no significant deviations from this value. The hydrogen positions do not differ significantly from a radial distribution about the cage except for H(8) and H(2) which lie essentially in the facial B_3 and C_2B_2 planes respectively [planes (2) and (1), Table 6]. Neither of these deviations from an idealised radial distribution can be attributed directly to packing effects (see below), and while it is tempting to attach significance to the position of H(8), that of H(2) is not easily rationalised, and the positions of both, along with the e.s.d.s of the hydrogen-atom parameters in general, must be viewed with some scepticism.

Metal–cage interaction. The mercury atom lies on the cage pseudo-mirror plane [plane (4), Table 6] to within 0.033 Å, with Hg–B(8) 2.20(1), Hg–B(7,4) 2.52(1), 2.50(1) Å, and Hg–C(1,2) 2.89(1), 2.91(1) Å. The metal cage distances thus fall into a new category, easily distinguishable from the symmetrically bonded d^6, d^7 $B_9C_2^{1,2}M^3$ structures such as $[B_9C_2^{1,2}\{Re(CO)_3\}^3H_{11}]^-$ (ref. 12) and the distorted d^8,d^9 structures such as $B_9C_2^{1,2}[Au(S_2CNEt_2)]^3H_{11}$ (ref. 5) where the M–C distances are much greater than the three similar M–B separations.

Phosphine mercury group. The phenyl-ring carbon

atoms are identified by C(ij) where i is the ring number (2—4) and j corresponds to sequential numbering of the ring vertices with $j = 1$ assigned to atoms bound to phosphorus. The apparently short C–C distances may be due to thermal motion [average U_{ii} values ranging from 0.034 Å^2 for U_{11} (ring 2) to 0.052 Å^2 for U_{33} (ring 4)], or more probably to deficiencies in the data, although only C(35)–C(36) differs significantly from the standard value of 1.395 Å and even this is only true if the value is rounded off from 1.395(12) Å. The rings themselves are planar to within 0.007, 0.005, and 0.014 Å for rings 2, 3, and 4 respectively, with the phosphorus atom lying out of these planes by 0.005, 0.182, and 0.041 Å. Similar distortions exist in PPh_3 itself,[15] and in the four-co-ordinate mercury(II) compound $[Hg(SCN)_2(PPh_3)_2]$.[16]

The Hg–P bond distance [2.393(2) Å] is in good agreement with the sum of covalent radii of 1.30 + 1.10 Å = 2.40 Å.[17,18] There are a few experimental values for mercury(II)–phosphorus distances in a distorted tetrahedral environment, values ranging from 2.487(3), 2.489(3) Å in the HgP_2S_2 unit in $[Hg(SCN)_2(PPh_3)_2]$ [16] to 2.52—2.56 Å in the HgP_4 unit in $PbHgP_{14}$,[19] but to the best of our knowledge no Hg–P bond distance for essentially linear mercury has previously been determined from X-ray structure analysis. The deviation of the P–Hg–B(8) angle from linearity (by 7.8°) is due almost solely to the phosphorus atom lying out of the cage pseudo-mirror plane by 0.39 Å, towards C(1) and B(4), and it seems probable that this is due to the molecular packing (see below) rather than to any asymmetric bonding of the mercury atom with respect to this pseudo-mirror plane. Steric effects may also be responsible for the variation in the Hg–P–C angle and perhaps, to a lesser extent, the C–P–C angles. The three P–C bond distances are normal, and agree well with those found in $[Hg(SCN)_2(PPh_3)_2]$.[16]

The dioxan of solvation and molecular packing. The dioxan molecule is situated on the centre of symmetry at 0,0,0 and adopts the normal chair configuration. The C–O bond distances agree well with expected values,[20] and that obtained for dioxan by electron diffraction [1.423(3) Å] [21] as do the interbond angles. The C–C distance is shorter, but not significantly so, than the expected [20] value of 1.54 Å and the electron-diffraction value of 1.523(5) Å.

The major role that the dioxan plays in the molecular packing is clearly evident from the contact distances given in Table 7, with close contacts developing to the cage and each of the phenyl groups. The lattice stabilisation is completed by additional cage–cage, cage–phosphine, and phosphine–phosphine contacts. The molecular packing is illustrated in Figure 2.

The number of possibly significant contacts provides a complex picture of a relatively crowded lattice, those listed in Table 7 representing three-dimensional stabilisation for each phenyl ring, the cage, and the dioxan. Each phenyl ring is locked in position by the cage, the dioxan, and neighbouring phosphine groups, in addition to the intraligand constraints in the phosphine itself. If the displacement of the phosphorus atom from the cage pseudo-mirror plane and the Hg–B(8) line, and the differing Hg–P–C angles, are caused by the packing, individual contacts involved are difficult to isolate since the phosphine ligand as a whole appears to be displaced. However, considering the sum of contacts, the stereochemistry is presumably the least sterically hindered for the bonding requirements and the mode of packing adopted, and a change such as to linearity of Hg, P, and B(8) would, while relieving some contacts,

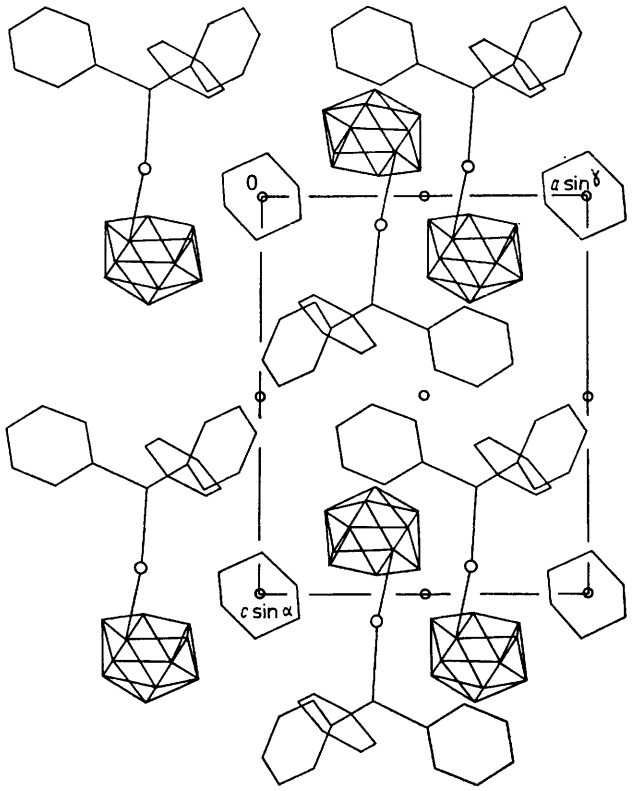

FIGURE 2 Molecular packing viewed parallel to b. The larger circles represent Hg and the smaller the projected crystallographic inversion centres

TABLE 7

Selected contact distances (Å); H–H <2.6, X–H <2.9, X–X <3.5 Å

Hg–H(22)	2.88	H(4)–H(521^{VII})	2.47
Hg–H(8^{I})	2.89	H(4)–H(512^{II})	2.40
		H(4)–C(51^{II})	2.83
H(5)–H(1^{II})	2.49		
		C(23)–O^{VII}	3.38
H(32)–H(10^{III})	2.54	H(23)–O^{VII}	2.63
H(25)–H(9^{III})	2.50	C(35)–O^{VIII}	3.45
H(43)–H(7^{IV})	2.57	H(35)–O^{VIII}	2.59
		C(43)–O	3.28
C(34)–H(24^{V})	2.76	H(36)–H(522^{IV})	2.58
H(34)–H(24^{V})	2.65		
H(45)–H(46^{VI})	2.59		
C(25)–H(45^{VI})	2.69		

Equivalent positions relative to the reference molecule at x, y, z:

I	$1-x, 1-y, -z$	V	$1-x, 1-y, 1-z$
II	$1-x, -y, -z$	VI	$1-x, -y, 1-z$
III	$x, y, 1+z$	VII	$1+x, y, z$
IV	$-x, 1-y, -z$	VIII	$x, 1+y, z$

cause overcrowding in other parts of the lattice. Thus, in viewing the structure as a whole, it seems likely that the non-bonded contacts given in Table 7 are in part responsible for the differing Hg–P–C angles, and perhaps the non-linearity of P–Hg–B(8), while the intraligand non-bonded contacts are responsible for the stereochemistry of the phosphine ligand itself.

Bonding and a discussion of the molecular distortions. Perhaps the most striking feature of the structure is the near linearity (172.2°) of the P–Hg–B(8) unit. The relatively short Hg–B(8) bond length (2.20 Å; sum of covalent radii = 2.18 Å) [17,18] the longer Hg–B(4,7) distances suggesting a weaker interaction, and the Hg–C(1,2) separations of 2.89, 2.91 Å (sum of covalent radii = 2.07 Å [18]) which constitute a weak or non-bonded interaction, suggest, in conjunction with the P–Hg–B(8) angle, that the complex is perhaps best described as pseudo-σ-bonded. Consistent with a σ-bonded description, the hydrogen atom attached to B(8) is displaced downwards by *ca.* 20° relative to the B(4,7,8) plane and towards this plane from a radially directed position although, as noted above, large uncertainties exist in the hydrogen-atom parameters.

The present structure is the first example of a metal derivative of $[B_9C_2^{7,8}H_{11}]^{2-}$ in which 'σ bonding' has been established. Such bonding had previously been suggested to occur in the reaction intermediate $B_9C_2^{7,8}H_{11}{\cdot}[Re(CO)_5]^-$, [1] and in the phenylmercury compound $[B_9C_2^{1,2}(HgPh)^3H_{11}]$ (through an Hg–C bond), and in view of the close similarity between metal compounds of the cyclopentadienyl and 7,8-dicarbaundecaboranyl ligands, it is perhaps surprising that no σ-bonded derivative of the latter had previously been structurally characterised. On the basis of the

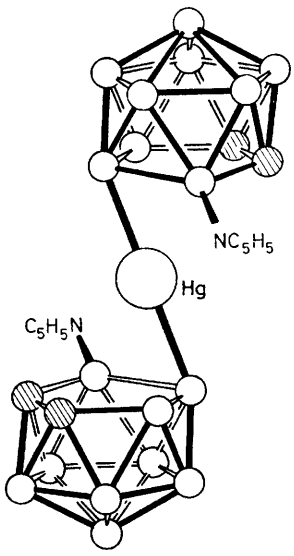

FIGURE 3 Proposed structure of $[Hg\{B_9C_2(NC_5H_5)H_{10}\}_2]$

present structure and similarities in the n.m.r. spectra discussed above, σ bonding between Hg and B(8) is also probable in both the $[B_9C_2(HgMe)H_{11}]^-$ and $[B_9C_2(HgPh)H_{11}]^-$ anions, and analogous structures seem likely for the gold(I) compound $B_9C_2[Au(PPh_3)](NC_5H_5)$ and the bis-cage derivative $[Hg(B_9C_2H_{10}{\cdot}C_5H_5N)_2]$

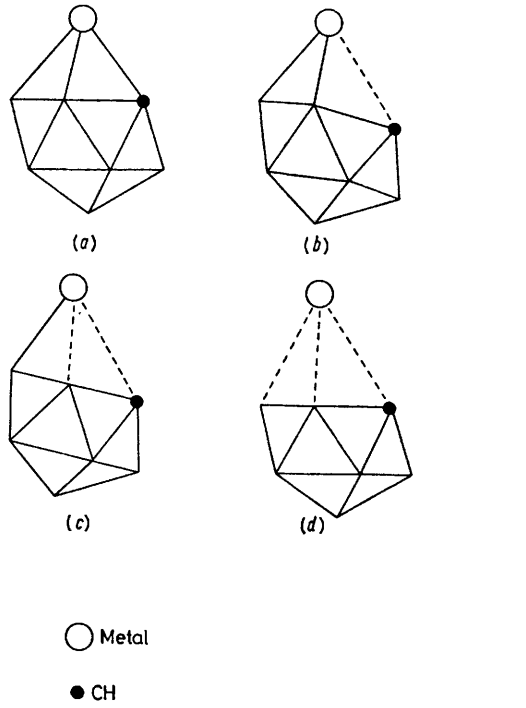

FIGURE 4 Metal–cage interactions in (*a*) $[B_9C_2^{1,2}\{Re(CO)_3\}^3H_{11}]^-$ (d^6, Re^I), (*b*) $B_9C_2^{1,2}[Au(S_2CNEt_2)]^3H_{11}$ (d^8, Au^{III}), (*c*) $B_9C_2^{1,2}$-$[Hg(PPh_3)]^3H_{11}$ (d^{10}, Hg^{II}), and (*d*) $[B_9C_2^{1,2}Tl^3H_{11}]^-$ ($d^{10}s^2$, Tl^I); projections are parallel to the cage C–C bond with all structures drawn to the same scale, and broken lines indicate weak or ionic bonding

(Figure 3). Since linear co-ordination is very much less common for Cu^I than for Au^I or Hg^{II}, however, a more symmetrical *closo* structure might be anticipated in $B_9C_2[Cu(PPh_3)]H_{10}{\cdot}C_5H_5N$ by analogy with the known η^5 structure of $[Cu(C_5H_5)(PPh_3)]$.[22] Interestingly, $[Au(C_5H_5)(PPh_3)]$ like $B_9C_2[Au(PPh_3)]H_{10}{\cdot}C_5H_5N$, is thought to contain a metal–ligand σ bond, with linear co-ordination about the gold atom.[23]

It is now possible to compare the structural changes which occur in the metal–cage fragment through an isoelectronic 18-electron series, namely $[B_9C_2\{Re(CO)_3\}H_{11}]^-$ (d^6, Re^I),[12] $B_9C_2[Au(S_2CNEt_2)]H_{11}$ (d^8, Au^{III}),[5] $B_9C_2[Hg(PPh_3)]H_{11}$ (d^{10}, Hg^{II}), and $[B_9C_2TlH_{11}]^-$ ($d^{10}s^2$, Tl^I).[6,9] It is apparent that the number of bonding interactions between the metal ions and the carbaborane cage progressively diminish as the electron density on the metal increases (Figure 4). In the rhenium compound, the three facial boron atoms are essentially equidistant from the metal (Re–B 2.32, 2.35, 2.35 Å), as are the two carbon atoms (Re–C 2.31 Å), and a similar relationship occurs in the gold compound with the important difference that the Au–C distances (2.78 Å) are significantly larger than the Au–B distances (av. 2.22 Å). This asymmetry in the bonding is extended in the present mercury derivative since only one boron of the facial B_3 fragment is now strongly bonded to the metal [Hg–

B(8) 2.20 Å]. In the thallium(I) species there is no bond distance which approximates to the sum of covalent radii, and the ion can be represented formally as an ion pair $Tl^+B_9C_2H_{11}^{2-}$.

There are also distinct changes in the framework geometry through the series, in general the largest significant differences occurring between the parameters of the bonded C_2B_3 faces (see description of structure), most noticeably the B–C separations and the bending of the face (0, 17, and 5° in the rhenium, gold, and mercury compounds respectively), and other bond lengths involving the carbon atoms. Finally, although the lower B_5 pentagonal girdle is essentially planar in both the rhenium and mercury derivatives it is significantly bent (by 9°) in the gold compound $B_9C_2[Au(S_2CNEt_2)]H_{11}$, with similar distortion in other d^8 derivatives such as $B_9C_2^{1,2}[Pt(PEt_3)_2]^3H_{11}$ (8°) [3] and the gold(III) sandwich $[3,3'\text{-}Au(B_9C_2^{1,2}H_{11})_2]^-$ (8°).

We have recently questioned whether the position of the metal atom in the distorted $B_9C_2^{1,2}M^3$ metallacarbaboranes is best described in terms of the long accepted ' slip ' definition by drawing attention to the pronounced non-planarity of the bonded C_2B_3 face.[5] Subsequently, a modified description of such structures has been devised to include a ' folding ' distortion of the C_2B_3 face. A ' slip ' parameter, Δ, has been related to the best least-squares plane through the *lower* B_5 pentagonal girdle B(5), B(6), B(11), B(12), B(9) and the ' slip ' defined as the distance which the central (metal) atom is displaced from the axis perpendicular to and passing through the centroid of this plane. The ' folding ' of the C_2B_3 face has been defined by two dihedral angles, ϕ and θ, but it has been pointed out that these terms do not bear any simple geometric relationship to Δ.[3]

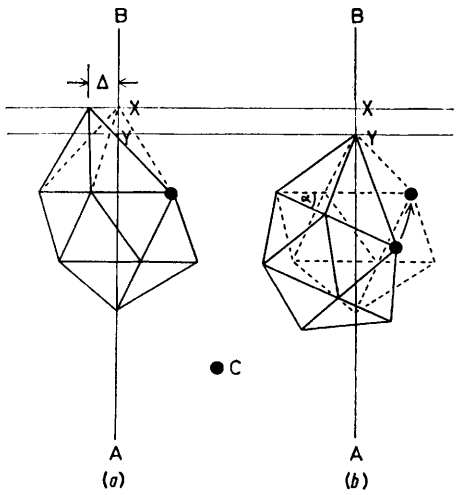

FIGURE 5 Examples of geometrical operations which produce a hypothetical symmetrically bonded ' parent ' from an observed structure: (*a*) observed structure (——), and metal position X in symmetrically bonded structure obtained *via* a ' slip ' of Δ; (*b*) observed structure (——), identical to that in (*a*), with metal at Y, and symmetrically bonded structure (– – –) obtained by a cage ' tilt ' of α. Both observed structures are drawn with an idealised cage and are identical. Both symmetrical ' parents ' are identical except for the position of the metal atom on the axis AB which is perpendicular to and symmetrically placed with respect to the C_2B_3 and B_5 planes

Although a combination of these three terms is useful for descriptive purposes, the basic difficulty in using any ' slip ' parameter remains, namely that such a term automatically implies and defines a unique ' parent ' compound (Δ = 0), even though such a ' parent ' is hypothetical. Such a ' parent ' has the central (metal) atom situated above the centroid of the pentagonal plane used to define Δ, and is presumed to have the metal positioned essentially symmetrically with respect to the atoms of *both* the C_2B_3 and B_5 planes *if* framework distortions, such as ' folding ' and ' interplane ' slip,[24] are removed. This is illustrated in Figure 5(*a*) and it should be noted that in the ' parent ' the central atom could be positioned at *any point*, compatible with reasonable metal–cage bonding distances, on the axis (AB), which passes through the centroids of, and is perpendicular to, the C_2B_3 and B_5 planes. Using the previous description involving ' slip ', the position is defined uniquely at X.

For the present structure, a Δ value [3] of 0.92 Å, with respect to the lower B_5 plane, gives symmetrical placement of the central atom at a point such as X [with Hg–B(8) 2.6, Hg–B(4,7) 2.5, Hg–C 2.4 Å], and a Δ value of 0.65 Å is required to give a similar placement with respect to the C_2B_3 face (with Hg–B = Hg–C = 2.5 Å). The so-called ' interplane slip ' (*ca.* 0.15 Å here),[3] that is the displacement of the bottom ' plane ' with respect to the bonded ' plane ', and other cage distortions which are not considered here, account for the discrepancy between the two Δ values. However, an alternative point, such as Y, may be obtained by a ' tilting ' of the cage towards the metal about an axis; for example, in the present structure, one passing through B(8) and parallel to the C–C bond, with a ' tilt ' of *ca.* 20° being required for the point Y [Figure 5(*b*)]. This yields a ' parent ' with Hg–B = Hg–C = 2.2 Å (*cf.* sum of covalent radii, Hg–B 2.18 Å; Hg–C 2.07 Å). Both descriptions, yielding the different points X and Y, therefore provide a symmetrically bonded ' parent ', and both are hypothetical since the ' parent ' is unknown.

While the ' slip ' notation remains useful, we have discussed ' tilt ' [25] as an alternative simply to highlight the uncertainty of the situation, and to clarify the implications of ' slip ' itself. Considering the available data, the most satisfactory and general description must remain one based on the various parameters involved in the metal–cage distances and the framework geometry.

Some modifications to the electron-counting rules, first postulated by Wade [26] and subsequently developed by several other workers,[27-29] which are widely used to predict the geometries of polyhedral frameworks, are necessary to deal with the series discussed above containing d^6 (Re^I), d^8 (Au^{III}), d^{10} (Hg^{II}), and $d^{10}s^2$ (Tl^I) metal ions. Wade has suggested that, in addition to the

' skeletal ' electron pairs of a polyhedral framework (n + 1 pairs for a *closo*, n + 2 for a *nido* system, *etc.*), up to three electron pairs may also be accommodated in non-bonding d orbitals on the metal. In the above series, therefore, as ligands are progressively removed from the metal, the metal clearly uses fewer orbitals for bonding the remaining ligands and the C_2B_9 cage, and the electron pairs previously assigned to the metal–ligand bonds appear to become associated with the MC_2B_9 polyhedron. Consequently if these electrons contribute to the total electrons within the polyhedral framework, then, on this basis, (n + 1), (n + 2), (n + 3), and (n + 4) skeletal electron pairs are associated with the presence of formal (d^0–d^6), d^8, d^{10}, and $d^{10}s^2$ ions respectively, leading to a progressive opening of the MC_2B_9 metallacarbaborane cage, as shown in Figure 4. It is essential, therefore, to consider the electron configuration of the metal in its formal oxidation state, at least for the heavier transition and post-transition elements, in the application of the electron-counting rules to metallacarbaborane frameworks. In a molecular-orbital (m.o.) bonding scheme the increasing electron density is assigned to metal–cage antibonding orbitals (e_1*, a_1*, where e_1* is derived from metal $d_{xz,yz}$ orbitals and a_1* from a metal s–p_z hybrid orbital).[30,31]

Finally, for the present structure, a complementary description of the bonding would be one arising principally from the overlap of a vacant metal *sp* hybrid orbital (giving linear co-ordination) with the ligand (PPh_3) and the occupied C_2B_9 cage e_1 orbital, which recent EHMO calculations have shown to be localised largely on the unique facial boron atom.[31]

EXPERIMENTAL

Instrumentation and techniques were as previously described.[25] The starting materials $[\{HgCl_2(PPh_3)\}_2]$,[32] $[AuCl(PPh_3)]$,[33] $[\{CuCl(PPh_3)\}_4]$,[34] $Tl[B_9C_2^{1,2}Tl^3H_{11}]$,[6] and $Na[B_9C_2^{7,8}(NC_5H_5)^9H_{10}]$ [10] were prepared by literature methods; elemental analyses were by B.M.A.C. Ltd., London. Boron-11 n.m.r. chemical shifts are given relative to $OEt_2{\cdot}BF_3$ with downfield shifts quoted as positive.

Preparations.—$B_9C_2^{1,2}[Hg(PPh_3)]^3H_{11}$ (1). The compound $[\{HgCl_2(PPh_3)\}_2]$ (5.34 g, 5 mmol) was suspended in dry thf (100 cm³) and $Tl[B_9C_2^{1,2}Tl^3H_{11}]$ (5.40 g, 10 mmol) added from a side-arm over *ca.* 15 min. After stirring for another 15 min, the pale yellow thallium(I) carbaborane had been replaced by a thick white precipitate which was filtered off and the filtrate evaporated to dryness under reduced pressure. The solid residue was taken up in the minimum of CH_2Cl_2 and the somewhat turbid solution filtered with charcoal to give a clear, very pale yellow solution. Slow addition of pentane afforded a colourless crystalline solid which was filtered off, washed with pentane, and dried *in vacuo*. The yield was 3.52 g (59%) of compound (1), m.p. 165 °C (Found: C, 40.6; H, 4.7; B, 16.1; Hg, 34.5. Calc. for $C_{20}H_{26}B_9HgP$: C, 40.3; H, 4.4; B, 16.3; Hg, 33.6%). The i.r. spectrum showed absorptions at 2 567s, 2 523vs, 2 493s, and 2 450m cm^{-1} in the ν(B–H) region (Nujol mull).

$[AsPh_4][B_9C_2^{1,2}(HgMe)^3H_{11}]$ (2). A 0.5 mol dm^{-3} aqueous solution of $K[B_9C_2H_{12}]$ (10 cm³, 5 mmol) was added to a cold (5 °C) solution of $[HgMe(O_2CMe)]$ (1.80 g, 6.5 mmol) and K[OH] (10 g) in water (100 cm³), and the solution warmed to room temperature with stirring. An aqueous solution of $[AsPh_4]^+$ was added dropwise with stirring, and the white precipitate filtered off, washed with ethanol and diethyl ether, and dried. Recrystallisation from acetone–hexane gave 2.17 g (60%) of compound (2) (Found: C, 45.6; H, 4.7; Hg, 28.1. Calc. for $C_{27}H_{34}AsB_9Hg$: C, 44.4; H, 4.7; Hg, 27.4%). The i.r. spectrum showed ν(B–H) at 2 560s, 2 536vs, 2 502s, 2 490s, 2 462s, and 2 408m cm^{-1} (Nujol mull).

$[NMe_4][B_9C_2^{1,2}(HgPh)^3H_{11}]$ (2a). The salt $Tl[B_9C_2^{1,2}Tl^3H_{11}]$ (2.70 g, 4.48 mmol) was added to a suspension of $[HgPh(NO_3)]$ (1.70 g, 5.01 mmol) in acetonitrile (50 cm³), and the reaction mixture stirred for 10 min. An aqueous solution of $[NMe_4]Br$ (5 g in 300 cm³) was added, and the precipitate filtered off and dried. Reprecipitation from thf–pentane gave 0.63 g (27%) of a white microcrystalline material, identified as $[NMe_4][B_9C_2^{1,2}(HgPh)^3H_{11}]$ by elemental analysis (Found: C, 30.0; H, 5.85; B, 20.1. Calc. for $C_{12}H_{28}B_8HgN$: C, 29.8; H, 5.8; B, 20.1%).

$B_9C_2^{1,2}[Au(PPh_3)]^3(NC_5H_5)^4H_{10}$ (3). The compound $[AuCl(PPh_3)]$ (0.47 g, 0.95 mmol) was added to a solution of $Na[B_9C_2^{7,8}(NC_5H_5)^9H_{10}]$ (0.94 mmol) in thf (25 cm³) and the mixture stirred for 20 min at room temperature, giving a yellow-brown solution and a grey precipitate. Filtration, followed by addition of pentane, yielded a yellow oil which crystallised on addition of a few drops of acetone. Recrystallisation from hot chloroform–hexane gave 0.31 g of bright yellow crystals of (3), m.p. 227 °C, 48% yield (Found: C, 45.0; H, 4.4; Au, 29.5; B, 14.1; N, 1.9. Calc. for $C_{25}H_{30}AuB_9NP$: C, 44.8; H, 4.5; Au, 29.4; B, 14.5; N, 2.1%). The i.r. spectrum showed ν(B–H) at 2 580s, 2 521vs, 2 478s, and 2 430m cm^{-1} (Nujol mull).

$B_9C_2^{1,2}[Cu(PPh_3)]^3(NC_5H_5)^4H_{10}$ (4). Reaction of $[\{CuCl(PPh_3)\}_4]$ (0.36 g, 0.25 mmol) with $Na[B_9C_2^{7,8}(NC_5H_5)^9H_{10}]$ [1.00 mmol in thf (30 cm³)] initially gave a dark red solution, which slowly (20 min) turned bright yellow and deposited a white solid. The solution was filtered, reduced to half-volume, and hexane (10 cm³) added slowly with stirring, giving bright yellow crystals of compound (4) (0.49 g, 91%), m.p. 196 °C (Found: C, 54.7; H, 5.3; B, 18.5; Cu, 12.5; N, 2.4. Calc. for $C_{25}H_{30}B_9CuNP$: C, 56.0; H, 5.6; B, 18.1; Cu, 11.9; N, 2.6%). The i.r. spectrum showed ν(B–H) at 2 568s, 2 522vs, and 2 455s cm^{-1} (Nujol mull).

$[3,3'\text{-}Hg\{B_9C_2^{1,2}(NC_5H_5)^4H_{10}\}_2]$ (5). Reaction of $HgCl_2$ (0.20 g, 0.74 mmol) with $Na[B_9C_2^{7,8}(NC_5H_5)^9H_{10}]$ (1.50 mmol) in thf (25 cm³) at room temperature, gave a pale yellow solution and a grey precipitate. The solution was filtered over Celite and pentane (25 cm³) added slowly with stirring, giving a pale yellow microcrystalline precipitate which was filtered off, washed with OEt_2, and dried *in vacuo*. The yield of complex (5) was 0.15 g (32%), m.p. 248 °C (Found: C, 26.7; B, 30.9; H, 32.0. Calc. for $C_{14}H_{30}B_{18}HgN_2$: C, 27.1; B, 31.4; Hg, 32.3%). The i.r. spectrum showed ν(B–H) at 2 540vs, br and 2 430m (sh) cm^{-1} (Nujol mull).

Crystal-structure Determination.—Complex (1) crystallised well from dichloromethane–hexane or thf–hexane, but on removal of the supernatant the crystals rapidly disintegrated due to loss of solvent of crystallisation. The complex could be obtained solvent-free from chloroform–hexane, but crystals were invariably twinned. Finally, single crystals of a somewhat thermally unstable 0.5-dioxan

solvate were obtained by slow addition of diethyl ether to a solution of (1) in acetone–1,4-dioxan (2 : 1).

The difficulty in producing crystals suitable for *X*-ray examination, and the apparent temperature instability of those finally obtained, led to a single crystal of the dioxan solvate of complex (1) being mounted and immediately transferred to a Syntex $P2_1$ four-circle diffractometer, with a low-temperature device (N_2 stream) already in operation at a steady-state temperature, *ca.* 213 K. Examination of several of the remaining good-quality crystals revealed them to be colourless plates, subsequently found to be bounded by (110), (010), (001) and the centrosymmetrically related planes. Of those examined the largest had dimensions *ca.* 0.015 × 0.015 × 0.006 cm, and all were noticeably smaller than that selected for the *X*-ray study. Optical examination using polarised light suggested that the crystal system might be triclinic.

Automatic centring on 15 reflections ($5 < 2\theta < 15°$), selected from a general rotation photograph taken using zirconium-filtered Mo-K_α radiation, established a type I reduced triclinic cell which was then used in a rapid collection (minimum speed 0.081 3° s^{-1}) of all unique intensities in the range $20 \leqslant 2\theta < 25°$. Accurate unit-cell parameters were then obtained from a least-squares analysis of the setting angles of 15 of the strongest of these intensities, well spread over the volume of collection, centred in the counter of the diffractometer.

Crystal data (213 K). $C_{20}H_{26}B_9HgP\cdot0.5C_4H_8O_2$, M = 639.3, Triclinic, space group $P\bar{1}$ established by the structure analysis, a = 10.913 5(17), b = 11.188 3(19), c = 12.007 1(18) Å, α = 83.50(1), β = 86.98(1), γ = 61.55(1)°, U = 1 280(4) Å^3, Z = 2, D_c = 1.657 g cm^{-3}, μ(Mo-K_α) = 60.8 cm^{-1}.

The data collection out to 2θ = 40° was completed in two shells separated at 35°. Collection in a third shell ($40 \leqslant 2\theta < 45°$) was nearing completion when a temporary cessation of the flow of gaseous nitrogen resulted in the total destruction of the crystal. Despite the incomplete data set and the absence of information necessary to compute an absorption correction, the decision to analyse the available data was subsequently vindicated by the structural information obtained.

Of the 2 829 independent intensities measured, 2 450 had $I_0 > 3\sigma(I_0)$ and were classified as observed, the θ—2θ scan method with variable scan width (0.9° below $K_{\alpha1}$ to 0.9° above $K_{\alpha2}$) and scan rate (0.016 7—0.488 3° s^{-1}) was employed. The standard deviation $\sigma(I_0)$ was calculated from $\sigma(I_0) = S[C + (BG/R^2)]^{\frac{1}{2}}$ where S is the scan speed, C the total scan count, BG the sum of the background counts taken at the extremes of the scan, and R (set to 0.5) the ratio of the total background to total scan counting times. Over the 125-h *X*-ray exposure, four reference reflections (010, $\bar{2}\bar{3}0$, 401, 642), remeasured after each block of 100, showed no significant variation. After local correction for Lorentz and polarisation effects, all computations were carried out on the CDC 7600 computer at the University of Manchester Computing Centre using the programs described in ref. 35.

Solution and refinement. The major peaks contained in a three-dimensional Patterson synthesis were consistent in both position and weight with Hg–Hg and Hg–P vectors in the space group $P\bar{1}$. The successful solution of the structure confirmed this choice of space group. A structure-factor calculation based on the mercury and phosphorus atoms with an arbitrary isotropic thermal parameter (B 3.0 Å^2) gave a residual $R[=\Sigma(|F_o| - |F_c|)/\Sigma|F_o|]$ of 0.37 for the observed reflections, which was reduced to 0.18 following three cycles of full-matrix least squares minimising $\Sigma w(|F_o| - |F_c|)^2$ with unit weights. All the remaining non-hydrogen atoms were located from a Fourier synthesis and were assigned B = 3.0 Å^2. The dioxan of solvation was centrosymmetrically positioned on 0,0,0. Least-squares refinement assuming an isotropic vibration model for all the non-hydrogen atoms reduced R to 0.070. Atomic scattering factors were taken from ref. 36. Three more cycles of least-squares refinement using anisotropic thermal parameters $U = \exp[-2\pi^2(U_{11}h^2a^{*2} \ldots + 2U_{23}klb^*c^*)]$ and anomalous scattering components [37] for Hg and P gave R 0.042. All the hydrogen atoms were strongly indicated in a difference-Fourier synthesis and were included in the model, with isotropic thermal parameters set at 120% of the converged isotropic equivalent of the atom to which they were bonded. The difference synthesis also contained large peaks (+2 to −2 e Å^{-3}) and sharp gradients in the region of the mercury atom, which were thought to be due mainly to the absence of an absorption correction. Least-squares refinement including all the parameters except the isotropic thermal parameters of the hydrogen atoms reduced R to 0.037. Atomic scattering factors for the hydrogen atoms were taken from ref. 38. Analysis of the data in ranges of $|F_o|$ and $(\sin\theta)/\lambda$ indicated that a weighting scheme of the form $w = [1 + b|F_o| + c(\sigma F)^2 + d(F_o)^4]^{-1}$ was suitable, the final term being used to downweight those reflections most obviously affected by absorption. The values of b, c, and d were 0.1, 2.0, and 0.3 × 10^{-6} respectively; least-squares refinement based on these values left R' $\{ = [\Sigma w(|F_o| - |F_c|)^2/\Sigma wF_o^2]^{\frac{1}{2}}\}$ unchanged at 0.046 and reduced the standard deviation of an observation of unit weight $\sigma_1 = [\Sigma w(|F_o| - |F_c|)^2/(m - n)]^{\frac{1}{2}}$ from 2.1 to 0.7. The standard deviations of the atomic co-ordinates were improved by *ca.* 10%. A weight analysis carried out *after* the final cycle of least squares showed maximum and minimum values of $w\Delta^2$ over the 12 ranges of $|F_o|$ of 0.46 and 0.34 and the weighting coefficients were left unaltered. The value of R remained at 0.037. A difference-Fourier synthesis based on $w\Delta F$ was computed, and the only deviations from a general background level of 0—5 e Å^{-3} using an arbitrary electron-density scale factor of 100 were two peaks of −40 and two of +30 in the region of the mercury atom and one of +20 in the region of B(1)–H(1). The behaviour of the atom H(1) was poor during further cycles of least squares, oscillating between two positions with a shift-to-error ratio in the y co-ordinate of 4.9 : 1 in each cycle. The average shift-to-error ratio was 0.12 : 1 for all the parameters and 0.9 : 1 for the non-hydrogen atom parameters with a maximum of 0.74 : 1 for the z co-ordinate of B(1). Further least-squares refinement was carried out with a damping factor of 0.5 for parameter shifts and the refinement converged with the B(1) and H(1) parameters reasonably stable. The final value of R was 0.37, wR was 0.45, and σ_1 was 0.69. The average shift-to-error ratio was 0.011 : 1 with a maximum of 0.078 : 1.

Observed and calculated structure factors and thermal parameters are listed in Supplementary Publication No. SUP 22417 (23 pp.).*

We thank the S.R.C. for grants in support of this work, Johnson, Matthey Ltd. for a generous loan of heavy-metal

* For details see Notices to Authors No. 7, *J.C.S. Dalton*, 1978, Index issue.

salts, and Dr. D. M. P. Mingos for preprints of his papers.

[8/1003 *Received* 31*st May*, 1978]

REFERENCES

[1] M. F. Hawthorne, D. C. Young, T. D. Andrews, D. V. Howe, R. L. Pilling, A. D. Pitts, M. Reintjes, L. F. Warren, and P. A. Wegner, *J. Amer. Chem. Soc.*, 1968, **90**, 879.
[2] L. F. Warren and M. F. Hawthorne, *J. Amer. Chem. Soc.*, 1970, **92**, 1157.
[3] D. M. P. Mingos, M. I. Forsyth, and A. J. Welch, *J.C.S. Chem. Comm.*, 1977, 605.
[4] L. F. Warren and M. F. Hawthorne, *J. Amer. Chem. Soc.*, 1968, **90**, 4823.
[5] H. M. Colquhoun, T. J. Greenhough, and M. G. H. Wallbridge, *J.C.S. Chem. Comm.*, 1976, 1019.
[6] J. L. Spencer, M. Green, and F. G. A. Stone, *J.C.S. Chem. Comm.*, 1972, 1178.
[7] H. M. Colquhoun, T. J. Greenhough, and M. G. H. Wallbridge, *Acta Cryst.*, 1977, **B33**, 3604.
[8] B. M. Mikhailov and T. V. Potapova, *Izvest. Akad. Nauk S.S.S.R., Ser. Khim.*, 1970, **11**, 2634.
[9] H. M. Colquhoun, Y. J. Greenhough, and M. G. H. Wallbridge, *J.C.S. Chem. Comm.*, 1977, 737.
[10] D. C. Young, D. V. Howe, and M. F. Hawthorne, *J. Amer. Chem. Soc.*, 1969, **91**, 859.
[11] M. F. Hawthorne and T. D. Andrews, *J. Amer. Chem. Soc.*, 1965, **87**, 2496.
[12] A. Zalkin, T. E. Hopkins, and D. H. Templeton, *Inorg. Chem.*, 1966 **5**, 1189.
[13] F. V. Hansen, R. G. Hazell, C. Hyatt, and G. D. Stucky, *Acta Chem. Scand.*, 1973, **27**, 1210.
[14] R. M. Wing, *J. Amer. Chem. Soc.*, 1967, **89**, 5599.
[15] J. J. Daly, *J. Chem. Soc.*, 1964, 3799.
[16] R. C. Makhija, A. L. Beauchamp, and R. Rivest, *J.C.S. Dalton*, 1973, 2447.
[17] D. Grdenić, *Quart. Rev.*, 1965, **19**, 303.
[18] L. Pauling, 'The Nature of the Chemical Bond,' Oxford University Press, 1960, ch. 7, p. 221.
[19] H. Krebs and Th. Lidwig, *Z. anorg. Chem.*, 1958, **294**, 257.
[20] L. E. Sutton, 'Tables of Interatomic Distances,' *Special Publ.*, The Chemical Society, London, 1965, no. 18.
[21] M. Davis and O. Hassel, *Acta Chem. Scand.*, 1963, **17**, 1181.
[22] F. A. Cotton and J. Takats, *J. Amer. Chem. Soc.*, 1970, **92**, 2353.
[23] R. Hüttel, V. Raffay, and H. Reinheimer, *Angew. Chem., Internat. Edn.*, 1967, **6**, 862.
[24] D. M. P. Mingos, M. I. Forsyth, and A. J. Welch, *J.C.S. Dalton*, 1978, 1363.
[25] H. M. Colquhoun, T. J. Greenhough, and M. G. H. Wallbridge, *J.C.S. Dalton*, 1978, 303.
[26] K. Wade, *Chem. Comm.*, 1971, 792; *Adv. Inorg. Chem. Radiochem.*, 1976, **18**, 1.
[27] R. E. Williams, *Adv. Inorg. Chem. Radiochem.*, 1976, **18**, 67.
[28] C. J. Jones, W. J. Evans, and M. F. Hawthorne, *J.C.S. Chem. Comm.*, 1973, 543.
[29] R. W. Rudolph, *Accounts Chem. Res.*, 1976, **9**, 446.
[30] D. M. P. Mingos, *J.C.S. Dalton*, 1977, 602.
[31] D. M. P. Mingos and M. I. Forsyth, *J. Organometallic Chem.*, 1978, **146**, C37.
[32] R. C. Evans, F. G. Mann, H. S. Peiser, and D. Purdle, *J. Chem. Soc.*, 1950, 1209.
[33] C. Kowala and J. M. Swan, *Austral. J. Chem.*, 1966, **19**, 547.
[34] F. Glockling and K. A. Hooton, *J. Chem. Soc.*, 1962, 2658.
[35] '*X*-Ray' 1972, Technical Report TR-192, ed. J. M. Stewart, Computer Science Centre, University of Maryland.
[36] D. T. Cromer and J. B. Mann, *Acta Cryst.*, 1968, **A24**, 321.
[37] D. T. Cromer and D. Liberman, *J. Chem. Phys.*, 1970, **53**, 1891.
[38] R. F. Stewart, E. R. Davidson, and W. T. Simpson, *J. Chem. Phys.*, 1965, **42**, 3175.